# *Article*

# Cytotoxicity and Leishmanicidal Activity of Isoniazid-Derived Hydrazones and 2-Pyrazineformamide Thiosemicarbazones

**Raquel S. Amim,[a] Gisele S. S. Firmino,[a] Ana C. P. D. Rego,[a] Adriane L. Nery,[b] Silvia A. G. Da-Silva,[b] Marcus V. N. de Souza,[c] Claudia Pessoa,[d] Jackson A. L. C. Resende,[e] José D. Figueroa-Villar[f] and Josane A. Lessa*[a]**

[a]*Departamento de Química Geral e Inorgânica, Instituto de Química, Universidade do Estado do Rio de Janeiro (UERJ), 20550-900 Rio de Janeiro-RJ, Brazil*

[b]*Laboratório de Imunofarmacologia Parasitária, Departamento de Microbiologia Imunologia e Parasitologia, Universidade do Estado do Rio de Janeiro (UERJ), 20551-030 Rio de Janeiro-RJ, Brazil*

[c]*Instituto de Tecnologia em Fármacos (Farmanguinhos), Fundação Oswaldo Cruz (Fiocruz), 21041-250 Rio de Janeiro-RJ, Brazil*

[d]*Laboratório de Oncologia Experimental, Universidade Federal do Ceará (UFC), 60430-270 Fortaleza-CE, Brazil*

[e]*Instituto de Química, Universidade Federal Fluminense (UFF), 24020-141 Niterói-RJ, Brazil*

[f]*Instituto Militar de Engenharia (IME), 22290-270 Rio de Janeiro-RJ, Brazil*

The isoniazid-derived hydrazones 2-pyridinecarbaldehyde- (HPCIH), 2-acetylpyridine- (HAPIH), 2-benzoylpyridine- (HBPIH), 2-pyridineformamide- (HPAmIH) and 2-pyrazineformamide- (HPzAmIH) isonicotinoyl hydrazones, as well as the pyrazinamide-derived thiosemicarbazones 2-pyrazineformamide- (HPzAm4DH), *N*(4)-methyl-2-pyrazineformamide- (HPzAm4M), *N*(4)-ethyl-2-pyrazineformamide- (HPzAm4E) and *N*(4)-phenyl-2-pyrazineformamide- (HPzAm4Ph) thiosemicarbazones, were assayed for their action against intracellular amastigote form of *Leishmania (Viannia) braziliensis* strains and the glioblastoma multiforme (SF-295), colon adenocarcinoma (HCT-116), ovarian cancer (OVCAR-8) and acute myeloid leukemia (HL-60) human tumor cell lines. All compounds exhibited leishmanicidal effects, with concentrations at which 50% of parasites were inhibited ($IC_{50}$) in the 10.70-18.84 µM range. Moreover, the compounds were up to 30-fold less toxic to macrophages than to the parasites. Pyrazinamide-derived thiosemicarbazones proved to have poor activity against the tumor cell lines at 5 µg mL$^{-1}$, whereas, in general the isoniazid-derived hydrazones presented good activity, being HAPIH and HBPIH the most potent compounds ($IC_{50}$ = 0.42-1.5 µM).

**Keywords:** antileishmanial activity, cytotoxicity, isoniazid, hydrazone, thiosemicarbazone

## Introduction

Cancer is one of the leading causes of death worldwide, with about 14 million new cases and 8.2 million cancer related deaths in 2012. Africa, Asia and Central and South America together correspond to 70% of the world's deaths.[1] Although chemotherapy has been an important form of cancer treatment, it presents some challenges such as need to improve the selectivity of drugs and consequent reduction of undesirable side effects and the high incidence of cell resistance,[2] which demonstrate the urgency for the development of new anticancer agents.

Leishmaniases are another set of diseases that require attention. They are caused by protozoa of the genus *Leishmania*, and present a spectrum of clinical forms, including cutaneous, mucosal and disseminated and diffuse cutaneous leishmaniasis.[3] *Leishmania braziliensis* is one of the most important species that cause American tegumentary leishmaniasis and the major agent causing the

*e-mail: josane@uerj.br

mucosal forms in Brazil.[4] Although regarded as neglected disease, leishmaniasis occurs in 98 countries, with an annual incidence of 1 to 1.5 million people worldwide.[1,5] The treatment of leishmaniasis is restricted to a few drugs, quite costly and increasingly challenged by the development of parasite resistance.[6] In this scenario, the search for drugs that are less toxic, more effective, and less costly is critical for the treatment of leishmaniasis in endemic countries.

Hydrazones and their thiosemicarbazone derivatives constitute a class of chelating agents which present antileishmanial[7-9] and cytotoxic[10,11] activities, among others.[12-14] There are a few works on antileishmanial activity of hydrazones and their thiosemicarbazone derivatives, whereas their potential as anticancer agents has been extensively investigated. 3-Aminopyridine-2-carboxaldehyde thiosemicarbazone (triapine), for example, is one promising candidate for anticancer drug, which is in clinical trial for the treatment of some kinds of cancer, such as pancreatic, cervical and ovarian.[15] We recently demonstrated that 2-acetylpyridine thiosemicarbazones present cytotoxic activity in nanomolar doses against malignant gliomas.[16] It has been proposed that the mechanism of anticancer action of thiosemicarbazones involves inhibition of ribonucleoside diphosphate reductase (RDR), a rate-limiting enzyme in DNA syntheses, which catalyzes the conversion of ribonucleotides into deoxyribonucleotides.[14]

In this work, the isoniazid (INH)-derived hydrazones 2-pyridinecarbaldehyde- (HPCIH, **1**),

2-acetylpyridine- (HAPIH, **2**), 2-benzoylpyridine- (HBPIH, **3**), 2-pyridineformamide- (HPAmIH, **4**) and 2-pyrazineformamide- (HPzAmIH, **5**) isonicotinoyl hydrazones, as well as the pyrazinamide (PZA)-derived thiosemicarbazones 2-pyrazineformamide- (HPzAm4DH, **6**), N(4)-methyl-2-pyrazineformamide- (HPzAm4M, **7**), N(4)-ethyl-2-pyrazineformamide- (HPzAm4E, **8**) and N(4)-phenyl-2-pyrazineformamide (HPzAm4Ph, **9**) thiosemicarbazones (Figure 1), were assayed for their action against *Leishmania (Viannia) braziliensis* strains and the glioblastoma multiforme (SF-295), colon adenocarcinoma (HCT-116), ovarian cancer (OVCAR-8) and acute myeloid leukemia (HL-60) human tumor cell lines. Cytotoxicity of **2** against SK-N-MC (human neuroepithelioma cell line) has been demonstrated by Bernhardt *et al.*,[17] which stimulated us to study the biological action of this and other compounds.

INH and PZA (Figure 1), along with ethambutol and rifampin, are some of the most important drugs used in the treatment of tuberculosis.[18] Mendez *et al.*[19] revealed that PZA displays *in vitro* antileishmanial activity on both promastigotes and amastigotes forms of *Leishmania major* with half maximal inhibitory concentration ($IC_{50}$) of 16.1 and 8.2 µM, respectively, after 48 h treatment. Moreover, PZA dramatically decreased lesion development and the parasite burden in C57BL/6 mice infected with the parasite.[19] Thus, we have been interested in evaluating the effects of structural modification of PZA, as well as INH, by including a hydrazone or thiosemicarbazone scaffold on its antileishmanial action.
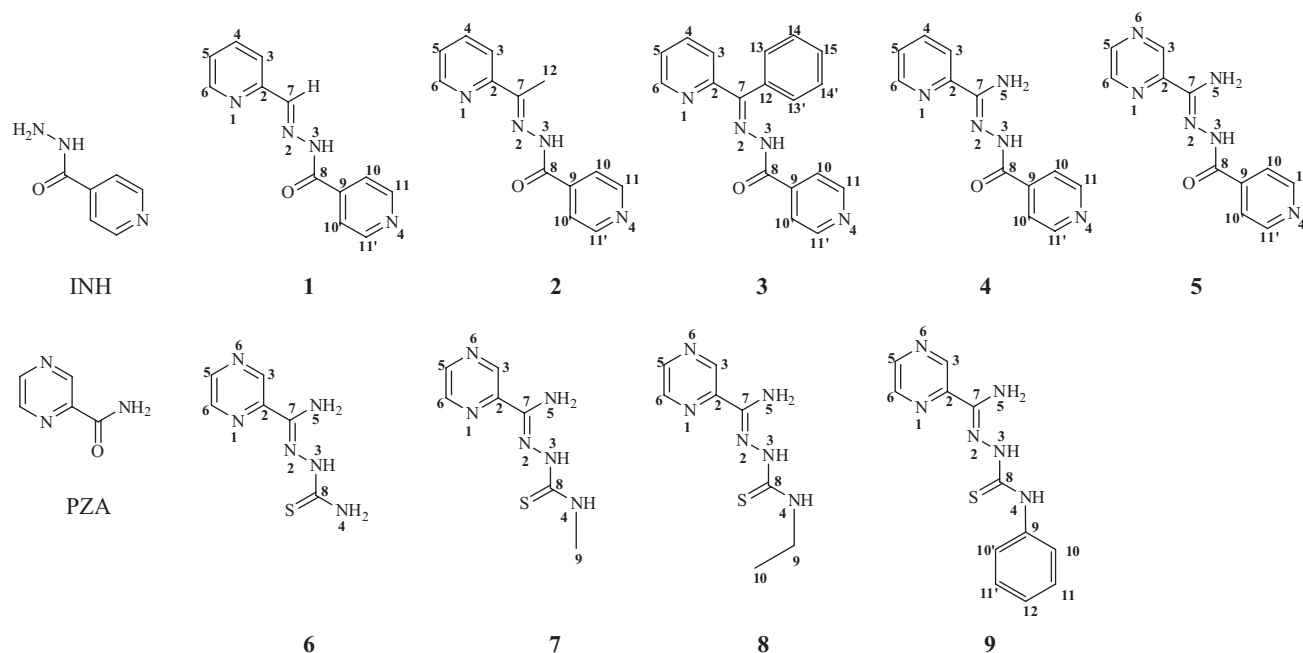


**Figure 1.** Structures of isoniazid (INH), pyrazinamide (PZA) and their derivatives **1-9**.

## Experimental

### Physical measurements

All common chemicals were purchased from Aldrich and used without further purification. Melting points were determined on a Uni-Melt capillary melting point apparatus (Arthur Hoover Thomas Company). Infrared (IR) spectra were recorded on a Perkin Elmer Fourier transform infrared (FTIR) Spectrum GX spectrometer using KBr plates (4000-400 cm⁻¹). Electronic spectra were recorded on an Agilent Technologies 8453 spectrophotometer at room temperature, using spectrophotometric grade solvents (dimethylformamide (DMF) or dimethylsulfoxide (DMSO)). Nuclear magnetic resonance (NMR) spectra were obtained on a Varian multinuclear UNITY-300 (600 MHz), for compounds **1-3** and **5-9**, or on a Bruker (400 MHz) spectrometer, for compound **4**, using DMSO-$d_6$ as solvent and tetramethylsilane (TMS) as internal reference. The ¹H resonances were assigned based on chemical shifts and multiplicities of ¹H NMR and 2D NMR correlation spectroscopy (COSY). The carbon type (C, CH$_x$) was determined by using attached proton test (APT) experiments. Assignments of the protonated carbons were made by 2D heteronuclear single quantum coherence (HSQC). Information on the configurational arrangement of compound **4** was obtained by using nuclear Overhauser effect spectroscopy (NOESY) experiment. High resolution mass spectra of the novel compounds in methanol solution were obtained in the negative ion mode on a Bruker micrOTOF-Q II electrospray ionization-tandem quadrupole-time-of-flight (ESI-Qq-TOF) (for compounds **8** and **9**) or in the positive ion mode on a Bruker TOF Compact Electrospray (for compound **4**) instrument.

### Synthesis of isoniazid and/or pyrazinamide-based molecules

Synthesis of HPCIH (**1**),[20] HAPIH (**2**)[17] HBPIH (**3**),[17,21] HPzAmIH (**5**)[22] as well as HPzAm4DH (**6**)[23] and HPzAm4M (**7**)[23] are described in the literature. IR and NMR data were compatible with the proposed structures (Supplementary Information).

The novel compounds 2-pyridineformamideisonicotinoyl hydrazone (HPAmIH, **4**), *N*(4)-ethyl-2-pyrazineformamide-thiosemicarbazone (HPzAm4E, **8**) and *N*(4)-phenyl-2-pyrazineformamide-thiosemicarbazone (HPzAm4Ph, **9**) were prepared following the literature procedure for the reduction of 2-cyanopyridine and 2-cyanopyrazine.[24] Thus, sodium (0.0493 g, 2.1 mmol) was solubilized in 25 mL of dry methanol. 2-Cyanopyridine (1.249 g, 12.0 mmol, for production of compound **4**) or 2-cyanopyrazine (1.261 g, 12.0 mmol, for production of compounds **8** and **9**) was then added, and the mixture was stirred for 0.5 h. After that, for the production of **4**, **8** and **9**, equimolar amount of isoniazid (1.645 g), *N*(4)-ethyl-3-thiosemicarbazide (1.430 g) or *N*(4)-phenyl-3-thiosemicarbazide (2.006 g), respectively, was added in small portions over a period of 0.5 h. The mixture was refluxed for 4 h and stirred for 24 h. The resulting solids were then filtered off, washed with methanol followed by diethyl ether, and dried *in vacuo*.

### 2-Pyridineformamideisonicotinoyl hydrazone (**4**)

White solid; yield: 40%; m.p.: > 240 ºC; UV-Vis (DMSO) $\lambda_{max}$ / nm 325; IR (KBr) $\nu_{max}$ / cm⁻¹ 3392, 3180, 3133, 1546, 1621, 842, 804, 749; ¹H NMR (400 MHz, DMSO-$d_6$) $\delta$ (*E* isomer (90%)) 7.03 (s, 2H, N5H$_2$), 7.51 (m, 1H, H5), 7.82 (s, 2H, H10), 7.92 (t, 1H, *J* 7.5 Hz, H4), 8.18 (d, 1H, *J* 7.8 Hz, H3), 8.62 (d, 1H, *J* 4.4 Hz, H6), 8.73 (d, 2H, *J* 5.6 Hz, H11), 10.41 (s, 1H, N3H); $\delta$ (*Z* isomer (10%)) 6.83 (s, 2H, N5H$_2$), 7.42 (m, 1H, H5), 7.71 (d, 2H, *J* 4.2 Hz, H10), 7.66-7.72 (m, 1H, H4), 7.77-7.85 (m, 1H, H3), 8.56 (d, 1H, *J* 4.7 Hz, H6), 8.75-8.70 (m, 1H, H11), 10.63 (s, 1H, N3H); ¹³C NMR (100 MHz, DMSO-$d_6$) $\delta$ (*E* isomer (90%)) 120.83, 121.70, 124.98, 137.01, 141.54, 148.16, 149.32, 149.99, 150.37, 161.34; $\delta$ (*Z* isomer (10%)) 120.08, 123.18, 124.57, 136.96, 142.36, 143.69, 148.07, 149.41, 150.16, 167.19; ESI-TOF calcd. for $C_{12}H_{12}N_5O$ [M]⁺: 242.1042; found: 242.1044.

### *N*(4)-Ethyl-2-pyrazineformamide thiosemicarbazone (**8**)

Yellow solid; yield: 50%; m.p.: 180-183 ºC; UV-Vis (DMF) $\lambda_{max}$ / nm 354, 1.80 × 10⁵; IR (KBr) $\nu_{max}$ / cm⁻¹ 3439, 3342, 3327, 3149, 2964, 1655, 1537, 778, 566; ¹H NMR (600 MHz, DMSO-$d_6$) $\delta$ 1.14 (t, 3H, *J* 7.1 Hz, CH$_3$), 3.60 (m, 2H, CH$_2$), 6.94 (s, 2H, N5–H), 8.49 (t, 1H, *J* 6.0 Hz, N4–H), 8.59 (m, 1H, H5), 8.66 (d, 1H, *J* 2.7 Hz, H6), 9.70 (d, 1H, *J* 1.8 Hz, H3), 10.09 (s, 1H, N3–H); ¹³C NMR (150 MHz, DMSO-$d_6$) $\delta$ 14.83, 38.18, 140.25, 142.55, 143.63, 144.60, 145.80, 176.02; ESI-TOF calcd. for $C_8H_{11}N_6S$ [M]⁺: 223.0766; found: 223.0991.

### *N*(4)-Phenyl-2-pyrazineformamide thiosemicarbazone (**9**)

Yellow solid; yield: 85%; m.p.: 180-182 ºC; UV-Vis (DMF) $\lambda_{max}$ / nm 358, 1.68 × 10⁵; IR (KBr) $\nu_{max}$ / cm⁻¹ 3414, 3275, 3225, 3165, 3028, 2962, 1658, 1545, 744, 594; ¹H NMR (600 MHz, DMSO-$d_6$) $\delta$ 7.14 (s, 2H, N5–H), 7.19 (m, 1H, H12), 7.36 (m, 2H, H10), 7.58 (m, 2H, H11), 8.63 (m, 1H, H5), 8.69 (d, 1H, *J* 2.3 Hz, H6), 9.85 (d, 1H, *J* 1.4 Hz, H3), 10.01 (s, 1H, N4–H), 10.52 (s, 1H, N3–H); ¹³C NMR (150 MHz, DMSO-$d_6$) $\delta$ 125.07, 126.01, 127.90, 130.34, 141.11, 142.59, 143.96, 144.91, 145.54, 175.11;

ESI-TOF calcd. for $C_{12}H_{11}N_6S$ $[M]^+$: 271.0766; found: 271.0984.

### X-Ray diffraction analysis

Single crystals of $[H_2PCIH]NO_3 \cdot H_2O$ (**1a**) and HPzAm4E (**8**) were obtained by slow evaporation of **1** and **8** in an ethanolic solution, in the presence and absence of nitrate, respectively. Data were collected at room temperature on a Bruker D8 VENTURE equipped with Mo Kα high-brilliance microfocus source (IμS) radiation ($\lambda = 0.71073$ Å) and a PHOTON 100 CMOS detector. The instrument was controlled with the APEX2 software package.[25] Data were processed using the integrated plug-in in the controlling software package (SAINT),[25] and corrected for absorption by the multiscan semi-empirical method implemented in SADABS.[25] Using Olex2,[26] the structure was solved with the SHELXS-97[27] structure solution program using direct methods and refined with the SHELXL-2013[27] refinement package using least squares minimization. Positional and anisotropic atomic displacement parameters were refined for all non-hydrogen atoms. Hydrogen atoms were placed geometrically and the positional parameters were refined using a riding model.

### Leishmanicidal activity

Antileishmanial activity studies were performed against intracellular amastigote forms of *Leishmania (Viannia) braziliensis* (MCAN/BR/98/R619). For this, resident macrophages were obtained from peritoneal cells of Swiss Webster mice after a peritoneal injection of 5 mL of Roswell Park Memorial Institute (RPMI) medium. For adherence, the peritoneal cells ($2 \times 10^6$ *per* mL) were plated onto glass coverslips placed within the wells of a 24-well culture plate (0.5 mL well$^{-1}$) and incubated at 37 °C in 5% $CO_2$ for 1 h. After removing the non-adherent cells, the monolayers of macrophages were infected with promastigotes of *L. braziliensis* (ratio of 5 promastigotes for each macrophage) for 4 h at 37 °C and 5% $CO_2$. The infected macrophages were washed and incubated with different concentrations of the tested compounds in RPMI medium supplemented with 10% of fetal bovine serum for 48 h at 37 °C and 5% $CO_2$. Each compound was previously dissolved in DMSO (stock solution). The final concentration of DMSO in the RPMI culture medium was kept below 0.3% (v/v). Controls were incubated with medium alone or with 0.3% of DMSO. The monolayers were then stained with Giemsa stain, and at least 100 infected macrophages *per* sample were counted under optical microscopy. After that, the infection index (% infected macrophages × number of

amastigotes / total number of macrophages) was calculated. $IC_{50}$ was determined by logarithmic regression analysis using GraphPad Prism 5. All assays were performed in at least three replicates and the results are shown as mean of three independent experiments.

To evaluate the toxicity of INH and PZA derivative molecules on mammalian cells, monolayers of murine macrophages ($4 \times 10^6$ in 200 μL) were incubated with the compounds (1.5-400 μmol L$^{-1}$) dissolved in RPMI medium supplemented with 10% of fetal bovine serum for 48 h at 37 °C and 5% $CO_2$. Controls were treated with medium or 1% of DMSO (the major final concentration of the diluent). Viability of macrophages was then assessed by measuring the mitochondrial dependent reduction of 3-(4,5-dimethyl-2-thiazol)-2,5-diphenyl-2*H*-tetrazolium bromide (MTT) to formazan. For this purpose, MTT (10 μL at 10 mg mL$^{-1}$) was added and monolayers of macrophages were incubated at 37 °C and 5% $CO_2$ for 3 h. The medium was removed and formazan crystals were dissolved in 180 μL of DMSO. The absorbance was read at 570 nm using a microplate spectrophotometer. The 50% of cytotoxic concentration ($CC_{50}$) was determined by logarithmic regression analysis using GraphPad Prism 5.

### Tumor cell culture and cytotoxic activity

SF-295, HCT-116, OVCAR-8 and HL-60 cancer cell lines, from the National Cancer Institute, were maintained in RPMI 1640 medium supplemented with 10% fetal bovine serum, 2 mmol L$^{-1}$ glutamine, 100 μg mL$^{-1}$ penicillin, and 100 μg mL$^{-1}$ streptomycin at 37 °C and 5% $CO_2$. Each compound was previously dissolved in DMSO (stock solution). The final concentration of DMSO in the RPMI culture medium was kept below 0.1% (v/v). PZA, INH and **1-9** (5 μg mL$^{-1}$) were incubated with SF-295, HCT-116 and OVCAR-8 cell lines, for 72 h. The cell viability was determined by reduction of MTT to formazan.[28]

Compounds that inhibited the proliferation in more than 50% were selected for determination of $IC_{50}$ against SF-295, HCT-116, OVCAR-8 and HL-60 tumor cell lines. To this end, 5-0.009 μg mL$^{-1}$ range for compound concentration was used. All experiments were performed in at least three replicates *per* compound and results shown are the average of three independent experiments.

## Results and Discussion

### Characterization of **4**, **8** and **9**

Compound **4**, as well as **5**, melts at a temperature above 240 °C. The similar hydrazones **1-3**, in turn, present

melting point lower than 200 ºC. The higher melting point values for **4** and **5** are probably due to the presence of $NH_2$ group, which may be involved in intermolecular hydrogen bonds. Vibrations in the infrared spectrum of **4** attributed to $\nu_a(NH_2)$, $\nu_s(NH_2)$ and $\nu(N–H)$ were observed at 3392-3133 $cm^{-1}$. Absorptions at 1659 and 1621 $cm^{-1}$ were attributed to $\nu(C=O)$ and $\delta(NH_2)$, respectively. These absorptions are shifted in relation to those present in the infrared spectrum of INH. One absorption at 1546 $cm^{-1}$ attributed to $\nu(C=N)$ was observed in the spectrum of **4**, but is absent in the IR spectrum of INH, suggesting that the condensation reaction took place, giving rise to an imine group in the molecular structure of **4**. The C–H out-of-plane bending ($\gamma$-CH) or ring bending ($\beta$-ring) absorptions from pyridine rings were present at 842, 804, 750 and 679 $cm^{-1}$.

Vibrations attributed to $\nu_a(NH_2)$, $\nu_s(NH_2)$ and $\nu(N–H)$ were observed at 3275-3414 $cm^{-1}$ in the IR spectra of **8** and **9**. Absorptions at 1655, 1533 and 778 $cm^{-1}$ in the spectrum of **8** were attributed to $\delta(NH_2)$, $\nu(C=N)$ and $\nu(C=S)$, respectively. These bands were observed at 1658, 1545 and 748 $cm^{-1}$, respectively, in the spectrum of **9**. The in-plane deformation mode of the pyrazine ring was present at 566 and 594 $cm^{-1}$ in the spectra of **8** and **9**, respectively.

We observed duplicated signals in the $^1H$ and $^{13}C$ NMR spectra of **4**, suggesting a mixture of two isomers, with the major one accounting for 90%. An analysis of the $^1H$ NMR spectrum of **4** shows that the maximum difference in $\delta$ between the signals of the isomers is observed for C3H proton of the *ortho*-pyridine group ($\Delta(\delta H(3)) = 0.4$ ppm). For other protons of both pyridine rings, the difference in chemical shifts between the two isomers is significantly smaller and in general does not exceed 0.1 ppm. For the amines N3H and $N5H_2$, we observed a difference in $\delta$ of 0.22 and 0.20 ppm, respectively. In order to obtain more information about the identity of the isomers, NOESY analysis was performed (Supplementary Information). For the major isomer, we observed spatial interaction between $N5H_2$ and H3, as well as between N3H and $N5H_2$. These interactions were not observed for the minor isomer. Thus, according to the analysis, the major isomer adopts the *E* configuration in solution, whereas the minor one corresponds to the *Z* configurational isomer. The proposed arrangements justify the most significant differences observed between chemical shifts of C3H and amine groups in both isomers. NMR spectra of similar hydrazones with the same behavior in solution had previously been observed and duplicated signals had been attributed to the presence of *E* and *Z* configurational isomers in solution[22,29] (Figure S16).

Only one signal for each proton was observed in the $^1H$ NMR spectra of **8** and **9**. The N3H chemical shifts at 10.09 and 10.52 ppm for **8** and **9**, respectively, indicate the molecules adopt the *E* configuration. Chemical shifts higher than 175 ppm observed for the signals of C8 in both compounds are typical of C=S, which suggest the thiosemicarbazones are in the thione form in solution.[16]

### X-Ray diffraction analysis

X-Ray crystal data of compounds $[H_2PCIH]NO_3 \cdot H_2O$ (**1a**) and HPzAm4E (**8**) are summarized in Table S1. Selected intra-molecular bond distances and angles for **1a** and **8**, as well as for HBPIH (**3**),[21] HPzAm4DH·$H_2O$[23] and HPzAm4M·$2H_2O$[23] are given in Tables S2 and S3. Selected dihedral angles, hydrogen bond distances (Å) and angles (º) for **1a** and **8** are shown in Tables S4 and S5, respectively. The Oak Ridge thermal ellipsoid plot (ORTEP) representation of asymmetric unit, showing ellipsoids displayed at 50% probability level, is shown in Figure 2.
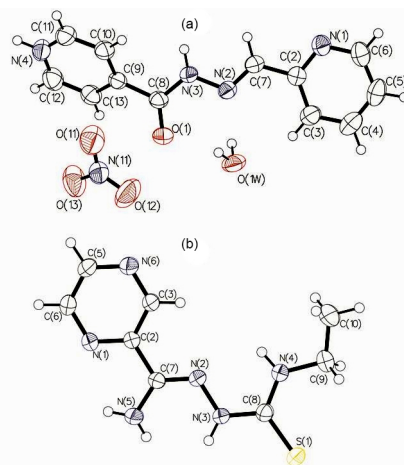


**Figure 2.** ORTEP representation of asymmetric unit of $[H_2PCIH]NO_3 \cdot H_2O$ (**1a**) (a) and HPzAm4E (**8**) (b), with ellipsoids at the 50% probability level.

The crystaline form of **1a** is a nitrate salt monohydrate (Figure 2a). The molecule is protonated at *p*-pyridine ring of the isoniazid bulk, which is hydrogen bonded with a nitrate ion (Figures 2a and 3). The C7–N2 and C8–O1 bond lengths, 1.220(2) and 1.272(2) Å, respectively, are expected for formally double bonds, whereas N2–N3 and N3–C8 lengths of 1.375(2) and 1.345(2) Å agree with the single character of these bonds.[21] Thus, **1a** is in the keto form, the same tautomer observed in crystal structure of its analog HBPIH (**3**).[21] Both compounds present similar values of bond distances and bond angles. The dihedral angles C2–C7–N2–N3 and N2–N3–C8–O1 are 178.83(18) and −1.8(3)º, respectively, for **1a** and suggest the molecule is in the *EZ* conformation, in relation to the C2–C7 and N3–C8 bonds. HBPIH (**3**), in turn, adopts *ZZ* conformation, probably to minimize steric hindrance due to the benzoyl bulk.[21]
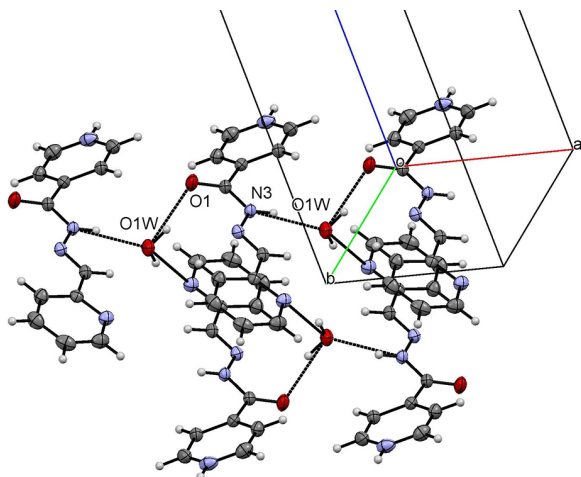
**Figure 3.** Hydrogen bond in [H$_2$PCIH]NO$_3$·H$_2$O (**1a**) along *a* axis.

Bond distances and angles for HPzAm4E (**8**) are similar to those ones observed in the crystal structures of HPzAm4DH·H$_2$O[23] and HPzAm4M·2H$_2$O.[23] N3–C8 and C8–S1 bonds of 1.359(2) and 1.6765(17) Å, respectively, are in agreement with the thione form for **8**.[16] According to values of N1–C2–C7–N2 and N2–N3–C8–S1 dihedral angles for **8**, the thiosemicarbazone adopts the *EE* conformation in relation to the C2–C7 and N3–C8 bonds (see Figure 2b). This conformation may occur, in part, as a result of the intramolecular N(4)–H(4)····N(2) hydrogen bond. Another relevant interaction, N(3)–H(3)····N(6)$^{[0.5 - x, -0.5 + y, 1.5 - z]}$, forms the chain along *b* axis (Figure 4). In the supramolecular arrangement, the inverse dimers as result of the N(5)–4H(5B)····S1$^{[-x, -y + 1, -z + 1]}$ interaction are also observed.

### Antileishmanial activity

To evaluate the antileishmanial effect of compounds we used intracellular amastigote of *L. braziliensis*, since this parasite form is relevant for infected host treatment. All the compounds, including PZA and INH, reduced the infection index in relation to untreated control ($p < 0.05$), with IC$_{50}$ in the 33.36-10.70 µM range (Table 1). The isoniazid-derived hydrazones **1**-**5** were as potent as INH, while the thiosemicarbazone derivatives were in general more active than PZA. HPzAm4M (**7**) (IC$_{50}$ = 10.70 ± 2.84 µM), for example, was about 3-fold more active than the original molecule PZA (IC$_{50}$ = 33.36 ± 7.60 µM).

Microscopic observation of stained infected macrophages (Figure 5) illustrates the antiparasitic activity of tested compounds without apparent toxicity to host cell. The treatment with 25 µmol L-1 of HPzAm4M (**7**) induces a major reduction in the number of amastigotes inside macrophages (Figure 5b) when compared to untreated control (Figure 5a). Under these experimental conditions, the antileishmanial effect of compounds was independent of nitric oxide production by infected macrophages (data not shown).

Meglumine antimonate (glucantime), a drug of choice for the treatment of leishmaniasis, was used as control. Its structure and composition is not completely understood and, in aqueous solution, it exists as a complex mixture in equilibrium.[30] Thus, the IC$_{50}$ value for glucantime was expressed as µg mL$^{-1}$ units. We found that all compounds are more potent against *L. braziliensis* than the antileishmaninal drug.

Toxicity studies of the tested compounds on macrophage allow us to evaluate its selectivity index (SI). INH, PZA and their derivatives were selectively active against intracellular amastigote of *L. braziliensis*. The compounds with better SI values are HAPIH (**2**, SI = 30.00) and HPzAm4DH (**6**, SI = 20.83). These results suggest the studied hydrazones and thiosemicarbazones have potential application as antileishmanial agents.
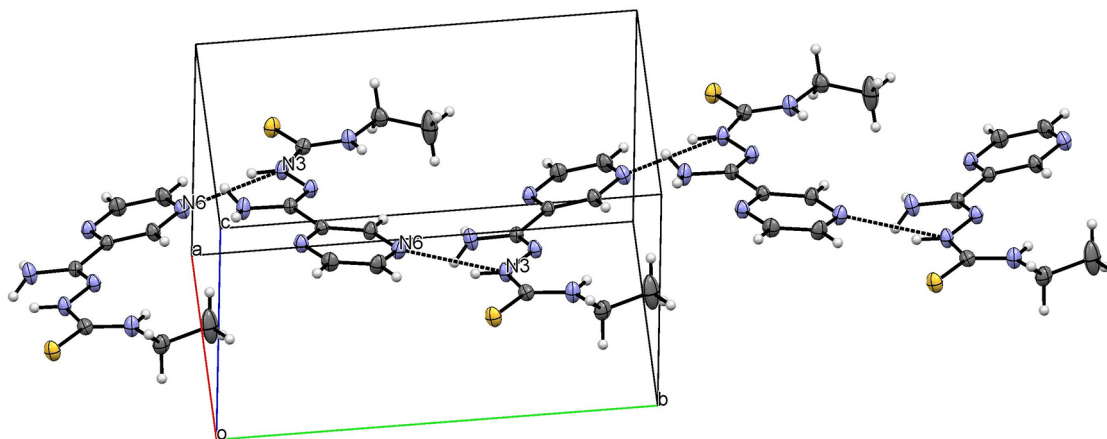


**Figure 4.** Hydrogen bond in HPzAm4E (**8**) along *b* axis.

**Table 1.** Data of toxicity of PZA and its derivatives **1-9** against *Leishmania braziliensis* ($IC_{50}$) and macrophages ($CC_{50}$) and the respective selectivity index

| Compound | $IC_{50} \pm SD$ / ($\mu g\ mL^{-1}$) | $IC_{50} \pm SD$ / $\mu M$ | $CC_{50} \pm SD$ / $\mu M$ | SI |
|---|---|---|---|---|
| INH | $2.33 \pm 0.60$ | $17.04 \pm 4.4$ | $336.4 \pm 21.74$ | 19.74 |
| HPCIH (**1**) | $3.25 \pm 0.79$ | $14.41 \pm 3.47$ | $273.8 \pm 136.47$ | 19.00 |
| HAPIH (**2**) | $4.01 \pm 0.49$ | $16.71 \pm 2.04$ | $501.38 \pm 124.80$ | 30.00 |
| HBPIH (**3**) | $4.86 \pm 2.55$ | $16.10 \pm 8.44$ | $126.24 \pm 59.46$ | 7.84 |
| HPAmIH (**4**) | $3.54 \pm 1.33$ | $14.66 \pm 5.53$ | $108.63 \pm 34.79$ | 7.41 |
| HPzAmIH (**5**) | $5.02 \pm 0.67$ | $20.75 \pm 2.76$ | $127.98 \pm 56.23$ | 6.17 |
| PZA | $4.11 \pm 0.94$ | $33.36 \pm 7.6$ | $414.2 \pm 48.21$ | 12.4 |
| HPzAm4DH (**6**) | $3.66 \pm 1.63$ | $18.67 \pm 8.28$ | $389 \pm 47.94$ | 20.83 |
| HPzAm4M (**7**) | $2.25 \pm 0.60$ | $10.7 \pm 2.84$ | $153.18 \pm 54.89$ | 14.31 |
| HPzAm4E (**8**) | $4.63 \pm 3.29$ | $20.63 \pm 14.69$ | $235.8 \pm 82.87$ | 11.43 |
| HPzAm4Ph (**9**) | $5.13 \pm 2.17$ | $18.84 \pm 7.99$ | $76.64 \pm 19.62$ | 4.05 |
| Glucantime | $337 \pm 94$ | – | $> 10$ ($mg\ mL^{-1}$) | – |

$IC_{50}$: Half maximal inhibitory concentration; SD: standard deviation; $CC_{50}$: half maximal cytotoxic concentration; SI: selectivity index ($CC_{50}$ / $IC_{50}$); INH: isoniazid; PZA: pyrazinamide.
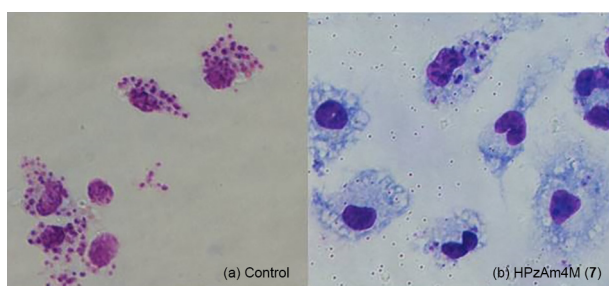


**Figure 5.** Aspect of infected macrophages: monolayers of murine macrophages were infected with promastigote form of *L. braziliensis* (ratio 5:1) during 4 h. After washing three times the infected monolayers were incubated with HPzAm4M (**7**) for 48 h. The monolayers were stained with Giemsa. The photographs show infected macrophages that (a) received no drug treatment (control) or (b) were treated with 25 μM of HPzAm4M (**7**).

## Activity against human tumor cell lines

The cytotoxic effects of the studied compounds at the 5 μg mL$^{-1}$ concentration are listed in Table 2. In general, the thiosemicarbazones exhibit low cytotoxicity against all cell lines, except HPzAm4E (**8**), which presents moderate action against HCT-116 and OVCAR-8 cells. HAPIH (**2**) and HBPIH (**3**) are the most potent hydrazones, whose activity is superior to INH.

Compounds **2** and **3** were selected for further determining $IC_{50}$ of SF-295, HCT-116, OVCAR-8 and HL-60 cells (Table 3). The hydrazones present similar activity against all cell lines and are only approximately 1.6

**Table 2.** Growth inhibition (%) of human tumor cell lines by INH, PZA and their derivatives **1-9**

| Compound | Growth inhibition[a] / % (mean ± SD) | | |
|---|---|---|---|
| | HCT-116 | OVCAR-8 | SF-295 |
| INH | $14.47 \pm 6.42$ | $-3.79 \pm 0.33$ | $21.01 \pm 2.85$ |
| HPCIH (**1**) | $15.74 \pm 3.82$ | $15.47 \pm 2.76$ | $-6.31 \pm 21.46$ |
| HAPIH (**2**) | $49.79 \pm 31.21$ | $94.53 \pm 3.46$ | $72.20 \pm 3.74$ |
| HBPIH (**3**) | $78.69 \pm 3.22$ | $98.63 \pm 3.18$ | $34.98 \pm 46.73$ |
| HPAmIH (**4**) | $22.37 \pm 8.91$ | $27.10 \pm 6.91$ | $38.39 \pm 0.72$ |
| HPzAmIH (**5**) | $15.88 \pm 0.27$ | $6.91 \pm 1.73$ | $2.60 \pm 0.79$ |
| PZA | ND[b] | ND[b] | ND[b] |
| HPzAm4DH (**6**) | $37.05 \pm 4.49$ | $7.74 \pm 3.87$ | $17.67 \pm 0.22$ |
| HPzAm4M (**7**) | $11.19 \pm 5.96$ | $23.67 \pm 10.09$ | $24.44 \pm 1.58$ |
| HPzAm4E (**8**) | $44.72 \pm 14.27$ | $52.60 \pm 8.43$ | $-7.64 \pm 42.77$ |
| HPzAm4Ph (**9**) | $15.36 \pm 6.77$ | $19.47 \pm 4.01$ | $29.02 \pm 1.15$ |

[a]Cell lines: HCT-116 (colon adenocarcinoma), OVCAR-8 (ovarian cancer) and SF-295 (glioblastoma multiforme); [b]ND: not determined. SD: standard deviation; INH: isoniazid; PZA: pyrazinamide.

**Table 3.** Cytotoxic activity ($IC_{50}$, in µM) of HAPIH (**2**) and HBPIH (**3**) against SF-295, OVCAR-8, HCT-116 and HL-60 tumor cell lines, in comparison with doxorubicin

| Compound | $IC_{50}$ / µM (confidence interval, 95%) | | | |
|---|---|---|---|---|
| | SF-295 | OVCAR-8 | HCT-116 | HL-60 |
| **2** | 1.44 (1.13 to 1.83) | 0.78 (0.72 to 0.88) | 0.82 (0.66 to 1.01) | 0.44 (0.04 to 0.49) |
| **3** | 1.53 (1.24 to 1.90) | 0.81 (0.69 to 0.96) | 0.90 (0.73 to 1.11) | 0.42 (0.37 to 0.48) |
| Doxorubicin | 0.42 (0.35 to 0.46) | 0.49 (0.31 to 0.56) | 0.23 (0.16 to 0.31) | 0.04 (0.02 to 0.04) |

$IC_{50}$: Half maximal inhibitory concentration; SF-295: glioblastoma multiforme; OVCAR-8: ovarian cancer; HCT-116: colon adenocarcinoma; HL-60: acute myeloid leukemia.

up to 10-fold less effective than the control (doxorubicin) in inhibiting the cell growth.

## Conclusions

PZA, INH and their derivatives exhibit leishmanicidal effects on *Leishmania braziliensis*. All compounds were more potent than glucantime and selectively active against intracellular amastigote of *L. braziliensis* in relation to macrophages.

Pyrazinamide-derived thiosemicarbazones have proved to have poor activity against SF-295, OVCAR-8 and HCT-116 cell lines. On the other hand, the isoniazid-derived hydrazones showed activity against the tumor cell lines at the tested concentration. The hydrazones HBPIH (**3**) and HAPIH (**2**) are the most efficient cytotoxic compounds, whose activities against the three cancer cell lines were higher than isoniazid. These compounds have also proved to be only approximately 1.6 up to ten times less effective than the control (doxorubicin) to inhibit the SF-295, OVCAR-8, HCT-116 and HL-60 tumor cell lines growth. Thus, the studies indicate the structural modification of isoniazid was an interesting strategy to improve its cytotoxicity against the tested cell lines.

## Supplementary Information

Supplementary information (spectra used for the identification of synthesized and novel compounds, as well as X-ray crystal data of [$H_2$PCIH]$NO_3 \cdot H_2O$ (**1a**) and HPzAm4E (**8**)) is available free of charge at http://jbcs.sbq.org.br as PDF file.

CCDC 1046288 and 1046289 contain supplementary crystallographic data for **1a** and **8**, respectively. These data can be obtained free of charge via http://www.ccdc. cam.ac.uk/conts/retrieving.html, or from the Cambridge Crystallographic Data Centre, 12 Union Road, Cambridge CB2 1EZ, UK; fax: (+44) 1223-336-033; or e-mail: deposit@ccdc.cam.ac.uk.

## References

1. http://www.who.int/cancer/en/ accessed in November 2015.

2. Shapira, A.; Livney, Y. D.; Broxterman, H. J.; Assaraf, Y. G.; *Drug Resist. Updates* **2011**, *14*, 150.

3. Rottini, M. M.; Amaral, A. C. F.; Ferreira, J. L. P.; Silva, J. R. A. S.; Taniwaki, N. N. T.; Souza, C. S. F.; D'Escoffier, L. N.; Souza, F. A.; Hardoim, D. J.; Costa, S. C. G.; Calabrese, K. S.; *Exp. Parasitol.* **2015**, *148*, 66.

4. Alvar, J.; Velez, I. D.; Bern, C.; Herrero, M.; Desjeux, P.; Cano, J.; Jannin, J.; den Boer, M.; *PLoS One* **2012**, *7*, 35671.

5. Tiuman, T. S.; Santos, A. O.; Ueda-Nakamura, T.; Dias Filho, B. P.; Nakamura, C. V.; *Int. J. Infect. Dis.* **2011**, *15*, 525.

6. Dumetz, M. F.; Roy, S.; Arevalo, A.; Ponte-Sucre, J.; Dujardin, J. C.; *Expert Rev. Anti-Infect. Ther.* **2014**, *12*, 937.

7. Muhammad, M.; Ismail, N. H.; Ali, M.; Khan, K. M.; Khan, W.; Kashif, S. M.; Asraf, M.; *Med. Chem. Res.* **2014**, *23*, 5282.

8. Carvalho, S. A.; Kaiser, M.; Brun, R.; Da Silva, E. F.; Fraga, C. A. M.; *Molecules* **2014**, *19*, 20374.

9. Britta, E. A.; Scariot, D. B.; Falzirolli, H.; Ueda-Nakamura, T.; Silva, C. C.; Dias Filho, B. P.; Borsali, R.; Nakamura, C. V.; Britta, M. C.; *BMC Microbiol.* **2014**, *14*, 236.

10. Soares, M. A.; Lessa, J. A.; Mendes, I. C.; Da Silva, J. G.; Santos, R. G.; Salum, L. B.; Daghestani, H.; Andricopulo, A. D.; Day, B. W.; Vogt, A.; Pesquero, J. L.; Rocha, W. R.; Beraldo, H.; *Bioorg. Med. Chem.* **2012**, *20*, 3396.

11. Markovíca, V.; Janićijević, A.; Stanojković, T.; Kolundžija, B.; Sladić, D.; Vujčić, M.; Janović, B.; Joksović, L.; Djurdjević, P. T.; Todorović, N.; Trifunović, S.; Joksovíca, M. D.; *Eur. J. Med. Chem.* **2013**, *64*, 228.

12. Maia, P. I. S.; Graminha, A.; Pavan, F. R.; Leite, C. Q. F.; Batista, A. A.; Back, D. F.; Lang, E. S.; Ellena, J.; Lemos, S. S.; Salistre-de-Araujo, H. S.; Deflon, V. M.; *J. Braz. Chem. Soc.* **2010**, *21*, 1177.

13. Santos, M. R. L.; Barreiro, E. J.; Braz-Filho, R.; Miranda, A. L. P.; *J. Braz. Chem. Soc.* **1997**, *8*, 471.

14. Beraldo, H.; Gambino, D.; *Mini-Rev. Med. Chem.* **2004**, *4*, 159.

15. http://www.clinicaltrials.gov/, ClinicalTrials.gov identifiers: NCT00288093, NCT02595879, NCT02466971, accessed in November 2015.

16. Lessa, J. A.; Mendes, I. C.; Da Silva, P. R.; Soares, M. A.; Santos, R. G.; Speziali, N. C.; Romeiro, N. L.; Beraldo, E. J.; Barreiro, H.; *Eur. J. Med. Chem.* **2010**, *45*, 5671.

17. Bernhardt, P. V.; Wilson, G. J.; Sharpe, P. C.; Kalinowski, D. S.; Richardson, D. R.; *JBIC, J. Biol. Inorg. Chem.* **2008**, *13*, 107.

18. Manjunatha, U. H.; Smith, P. W.; *Bioorg. Med. Chem.* **2015**, *23*, 5087.

19. Mendez, S.; Traslavina, R.; Hinchman, M.; Huang, L.; Green, P.; Cynamon, M. H.; Welch, J. T.; *Antimicrob. Agents Chemother.* **2009**, *53*, 5114.

20. Armstrong, C. M.; Bernhardt, P.; Richardson, V. P.; Chin, D. R.; *Eur. J. Inorg. Chem.* **2003**, *6*, 1145.

21. Ababei, L. V.; Kriza, A.; Musuc, A. M.; Andronescu, C.; Rogozea, E. A.; *J. Therm. Anal. Calorim.* **2010**, *101*, 987.

22. Glushkov, R. G.; Modnikova, G. A.; L'vov, A. I.; Krylova, L. Y.; Pushkina, T. V.; Solov'eva, T. A.; Gus'kova, N. P.; *Pharm. Chem. J.* **2004**, *38*, 16.

23. Castineiras, A.; Garcia-Santos, I.; Nogueiras, S.; Rodriguez-Gonzalez, I.; Rodriguez-Riobo, R.; *J. Mol. Struct.* **2014**, *1074*, 1.

24. West, D. X.; Swearingen, J. K.; Valdes-Martinez, J.; Hernandez-Ortega, S.; El-Sawaf, A. K.; Meurs, F. V.; Castineiras, A.; Garcia, I.; Bermejo, E.; *Polyhedron* **1999**, *18*, 2929.

25. Bruker AXS Inc.; *APEX2, SAINT, SADABS*; Bruker AXS Inc., Madison, 2014.

26. Dolomanov, O. V.; Bourhis, L. J.; Gildea, R. J.; Howard, J. A. K.; Puschmann, H.; *J. Appl. Crystallogr.* **2009**, *42*, 339.

27. Sheldrick, G. M.; *Acta Crystallogr., Sect. A: Found. Crystallogr.* **2008**, *64*, 112.

28. Mosman, T.; *J. Immunol. Methods* **1983**, *65*, 55.

29. Kovarikova, P.; Vavrova, K.; Tomalova, K.; Schongut, M.; Hruskova, K.; Haskova, P.; Klimes, J; *J. Pharm. Biomed. Anal.* **2008**, *48*, 295.

30. Frézard, F.; Martins, P. S.; Barbosa, M. C. M.; Pimenta, A. M. C.; Ferreira, W. A.; Melo, J. E.; Mangrum, J. B.; Demicheli, C.; *J. Inorg. Biochem.* **2008**, *102*, 656.